Chemical Engineering Journal 110 (2005) 41–56

Chemical Engineering Journal

www.elsevier.com/locate/cej

Behaviour of smooth catalysts at high reaction rates

Sergio D. Keegan [a,b], Néstor J. Mariani [a,b,*], Osvaldo M. Martínez [a,b], Guillermo F. Barreto [a,b]

[a] *Departamento de Ingeniería Química, Facultad de Ingeniería, Universidad Nacional de La Plata, La Plata, Argentina*
[b] *Centro de Investigación y Desarrollo en Ciencias Aplicadas "Dr. J.J. Ronco" (CINDECA), CONICET, Universidad Nacional de La Plata, Calle 47 No. 257, CP B1900AJK, La Plata, Argentina*

Received 1 December 2004; received in revised form 25 April 2005; accepted 29 April 2005

Abstract

In evaluating effective reaction rates in catalysts subject to heat and mass transport limitations, the size of the catalytic body is best defined by the so-called characteristic length ℓ, the ratio between catalyst volume and its external surface area, $\ell = V_p/S_p$. This result follows from the limiting behaviour at very high reaction rates, when the effective reaction rates are proportional to $1/\ell$ (e.g., Aris [R. Aris, The Mathematical Theory of Diffusion and Reaction in Permeable Catalysts, Oxford University Press, London, 1975.]) or, in dimensionless form, to the inverse of the Thiele modulus Φ. It is further known from simple geometrical shapes that a series solution can be written in terms of powers of $(1/\Phi)$ and that the second order term $[\text{in}(1/\Phi)^2]$ depends on the shape of the catalytic body. It is the aim of this paper to develop expressions of such second order term for 2D or 3D catalytic bodies showing arbitrary smooth external surfaces.

In a similar way as the first order term allows to define the proper size of a catalyst, the second order term provides a characterization for the catalyst shape. This and other applications of the second order term are discussed.
© 2005 Elsevier B.V. All rights reserved.

Keywords: Diffusion-reaction; Effectiveness factor; Catalytic reactions; Shape factor

1. Introduction

Except for the case of spheres, diffusive transport of reactants in most kind of commercial catalytic pellets proceeds along more than one spatial coordinate. The general case will be a 3D[1] problem (e.g., a trilobe pellet), while 2D problems will be frequent, mainly due to axisymmetry (e.g., circular cylinders) and will also apply for monolith reactors with catalytic washcoat on non-circular channels [2].

Numerical codes and computer facilities have been developed up to such an extent that 2D and 3D problems are not computationally challenging problems, provided that a few isolate calculations should be made. However, relatively novel catalytic reactors, as reverse-flow reactors and reactive distillation processes, or more sophisticated models for traditional reactors, including CFD (computational fluid dynamics) simulations, can demand thousands, or higher orders, of spatial and temporal discretization points, in which the effective reaction rates should be evaluated. In addition, the occurrence of multiple reactions will strongly enhance the computational demand.

It will be then highly desirable, or even necessary, to avoid the use of 2D or 3D computations. This is actually feasible, largely because it is a well-known fact that if the results from different catalytic bodies are compared in terms of the characteristic length $\ell = V_p/S_p$, the effect of the shape is tempered. Table 1 shows deviations between the behaviour of a slab (the simplest 1D geometry) and a circular cylinder of height/radius ratio = 1.7 (a 2D problem) compared at the same ℓ for different kinetics (precise definition of $r(Y)$ is given in the next section).

* Corresponding author. Tel.: +54 2214211353; fax: +54 2214254277.
E-mail address: nmariani@quimica.unlp.edu.ar (N.J. Mariani).

[1] "3D" means that no suitable coordinate system can be chosen to reduce from three the number of coordinate directions taken by the flux of reactants. 1D or 2D applies when either one or two suitable coordinate directions can be found (e.g., axisymmetric problems will be 2D and problems on a sphere will be 1D).

1385-8947/$ – see front matter © 2005 Elsevier B.V. All rights reserved.
doi:10.1016/j.cej.2005.04.013

Nomenclature

a	catalytic activity (dimensionless)
a_S	local catalytic activity on S_p (dimensionless)
C_j	molar concentration of species j (mol m^{-3})
h_i	$=\lvert\partial\mathbf{x}/\partial\xi_i\rvert$, scale factor in the coordinate direction ξ_i (dimensionless)
I_1	parameter defined in Eq. (13b) (dimensionless)
I_2	parameter defined in Eq. (19a) (dimensionless)
J_A	parameter defined in Eq. (1d) (mol m^{-1} s^{-1})
k_{ef}	effective thermal conductivity (W °C^{-1} m^{-2})
k_{mj}	local mass transfer coefficient of species j (m s^{-1})
ℓ	$=V_p/S_p$, characteristic length (m)
L	Laplacian operator (m^{-2})
$\mathbf{n}$	normal unit vector on S_p (dimensionless)
$\mathbf{N}_j$	molar flux of species j (mol m^{-2} s^{-1})
$\boldsymbol{q}$	heat flux (W m^{-2})
$r(Y)$	$=\pi_A(Y)/\pi_{AS}$, relative reaction rate (dimensionless)
$\mathbb{R}$	$= I_2/I_1$ (dimensionless)
R_{high}	overall consumption rate in the asymptotic regime (mol s^{-1})
R_a, R_b	principal radii of curvature (m)
S_p	external surface area of the catalytic body accessible to reactants (m^2)
T	temperature (K)
V_p	volume of the catalytic body (m^3)
$\mathbf{x}$	$=(x_1, x_2, x_3)$, Cartesian coordinate vector (m)
Y	dimensionless concentration defined in Eq. (1c)

Greek letters

γ	geometric parameter (dimensionless)
Γ	parameter defined in Eq. (21) (dimensionless)
Υ_n, Υ_a, Υ_b	curvatures defined in Eqs. (8), (9d) and (9e) (m^{-1})
Υ_S	sum of local principal curvatures on S_p defined in Eq. (14b) (m^{-1})
λ	global reaction scale, defined in Eq. (2d) (m)
λ_S	$= \lambda/a_S^{1/2}$, local reaction scale at S_p (m)
π_j	specific consumption rate of species j (mol m^{-3} s^{-1})
ν_j	stoichiometric coefficient of species j (dimensionless)
Φ	$=\ell(\pi_{AS}/J_A)^{1/2}$, Thiele modulus (dimensionless)
η	effectiveness factor (dimensionless)
κ_g	geodesic curvature (m^{-1})
κ	principal curvature (m^{-1})
ξ_i	coordinate in the direction i (m)
ζ	$=\xi_n/\lambda_S$, stretched coordinate (dimensionless)

Subscripts

av	average over S_p
a, b	directions of the lines of curvature
e	chemical equilibrium
F	average in the fluid phase
high	asymptotic regime
n	normal direction
S	external surface

Different readings can be made from the data in Table 1. Advocating the existence of other sources of uncertainty, as kinetics itself, the shape effect may be regarded as being tolerable for rough and fast estimations. However, when simulating a complex catalytic process, the magnitude of the task will prompt for eliminating as many sources of uncertainty and inaccuracies as possible. Within this frame, the foregoing data indicate that the effect of shape cannot be ignored and that in order to avoid 2D or 3D calculations it will be necessary to have available criteria to choose a suitable geometrical simplification.

A suitable geometric characterization of the catalyst shape can be obtained from the expansion of the effectiveness factor at high reaction rates. The second term in such an expansion has been clearly identified for 1D geometries. For the case of a single reaction and uniform activity (see e.g. [3–5]) the effectiveness factor η for high values of Thiele modulus Φ can be expressed as:

$$\eta = \frac{I_1}{\Phi}\left(1 - \frac{\mathbb{R}}{\Phi}\Gamma\right) + \dots \tag{1a}$$

$$\Gamma = \frac{\sigma}{\sigma + 1} \tag{1b}$$

where I_1 and $\mathbb{R}$ are coefficients depending on the type of kinetic law (all quantities in Eqs. (1a) and (1b) will be precisely defined in the next sections) and σ is the geometric parameter for simple geometries: $\sigma = 0$, 1, 2, for a slab, a long circular cylinder and a sphere, respectively.

This paper is devoted to the development of an expression for evaluating the geometrical parameter Γ for catalytic bodies showing smooth external surfaces of arbitrary shape. Such expression is not available in the open literature, to the best of our knowledge. The effect of a non-uniform field of

Table 1
Maximum relative difference (Δ) between the effectiveness factor of a slab (1D) and a circular cylinder of ratio height/radius = 1.7 (2D), compared at the same ℓ

$r(Y)$	Δ (%)
Y^2	18
Y	19
$Y^{1/2}$	22
1 (if $Y > 0$)	34
$36Y/(1+5Y)^2$	38

catalytic activity will be included in this task; hence Γ will account for both, geometrical and activity field effects.

Given the assumption of smooth external surfaces (i.e., without edges), it is convenient to consider briefly the relevance of practical catalysts showing this property. Structured catalysts [6] are probably the most important type of catalysts presenting smooth surfaces. In many instances, the catalyst is deposited on a thin and uniform layer and therefore they can be analysed as a 1D geometry. However, in monolithic reactors, the catalytic washcoat deposited on the wall of the channels can show uneven thickness, as for the usual triangular or squared cross-section channels. In these cases, the thickness at the corners can be an order of magnitude higher than on the sides of the channels, and a 2D analysis is definitely required.

Apart from spheres, most existing shapes of commercial particulate catalysts (pellets or tablets) correspond to cylinders with a variety of cross-section shapes. They do not show smooth external surfaces, due to the edges around the bases. Suitable values of Γ for geometries showing edges are obtained by adding a correction term to the expression here obtained. These results will be presented in a separate contribution.

In the next sections, the expression for Γ will be developed on the base of assuming that a single reaction takes place. Nonetheless, it is shown in Appendix C that the same expression holds up for a system with multiple reactions.

2. Problem statement

A single catalytic reaction and the following restrictions will be considered in most part of this contribution (the significance of these assumptions will be discussed later on):

(a) Uniform composition and temperature at the external surface of the catalyst.
(b) Constitutive equations for the fluxes (transport model) are isotropic and intrinsically independent of position inside the catalyst.

Under these conditions, the stoichiometric relations for fluxes inside the catalyst hold up irrespective of catalyst geometry and of the transport model employed to describe the fluxes inside the catalyst [7,8]. Thus, if A is the key species, that will be assumed to be the limiting reactant, $\mathbf{N}_j$ is the flux of a generic species j, and ν_j its stoichiometric coefficient, $\mathbf{N}_j = (\nu_j/\nu_A)\mathbf{N}_A$. One of these relations (say $j \equiv \mathrm{h}$) can be associated with the heat flux ($-\nu_\mathrm{h} \equiv$ reaction heat). Once a transport model (e.g., the dusty gas model) is chosen to express each $\mathbf{N}_j$ in terms of the gradients of all state variables, the stoichiometric relations can be integrated subject to pellet surface conditions, but independently of spatial coordinates, to relate the concentration of each species and temperature with the concentration of A, C_A. In turn, the chemical equilibrium condition will allow to evaluate the equilibrium set of variables attainable inside the catalyst, in particular the value $C_{A\mathrm{e}}$.

The above underlined procedure formally allows to choose C_A as the only independent state variable. All others will be expressed as a function of C_A. Hence, the consumption rate of A (π_A) can also be written as a function of C_A only. Note that $\pi_A(C_{A\mathrm{e}}) = 0$. We can also write, $\mathbf{N}_A = -D(C_A)\nabla C_A$, where D can be also expressed as a function of C_A only. Both π_A and D will further depend on the values of the state variables at the external surface and on the true transport coefficients, as defined by the transport model. The following change of variables (from C_A to Y) will be useful:

$$Y = \frac{1}{J_A}\int_{C_{A\mathrm{e}}}^{C_A} D(C_A)\,\mathrm{d}C_A \tag{1c}$$

$$J_A = \int_{C_{A\mathrm{e}}}^{C_{A\mathrm{S}}} D(C_A)\,\mathrm{d}C_A \tag{1d}$$

Hence, $\mathbf{N}_A = -J_A\nabla Y$. In turn, we can write $\pi_A = \pi_A(Y)$ and define $r = r(Y) = \pi_A(Y)/\pi_{A\mathrm{S}}$, where $\pi_{A\mathrm{S}}$ is the value of π_A at the external surface. As a consequence, $Y = 1$ and $r(1) = 1$ on the external surface. At equilibrium conditions (eventually, well inside the catalytic body): $Y = 0$; $r(0) = 0$.

The previous manipulations allow to transfer the stoichiometry and transport complexities to the evaluation of the dimensionless rate $r(Y)$. This is assumed to be accomplished as an initial step, independently of reaction/transport interactions within the domain of the catalyst geometry.

As an elementary example, for the simplest transport models $\mathbf{N}_j = -D_j\nabla C_j$, $\boldsymbol{q} = -k_\mathrm{ef}\nabla T$, with constant D_j and k_ef:

$$(C_j - C_{j\mathrm{S}}) = \frac{D_A}{D_j}\frac{\nu_j}{\nu_A}(C_A - C_{A\mathrm{S}});$$

$$(T - T_\mathrm{S}) = \frac{D_A}{k_\mathrm{ef}}\frac{(-\Delta H)}{\nu_A}(C_A - C_{A\mathrm{S}});$$

$$Y = \frac{C_A - C_{A\mathrm{e}}}{C_{A\mathrm{S}} - C_{A\mathrm{e}}}; \qquad J_A = D_A(C_{A\mathrm{S}} - C_{A\mathrm{e}})$$

The steady state conservation balance for species A can be written,

$$L(Y) = \frac{1}{\lambda^2}a(\mathbf{x})r(Y), \quad \text{on } V_\mathrm{p} \tag{2a}$$

$$Y = 1, \quad \text{on } S_\mathrm{p} \tag{2b}$$

$$\nabla Y = 0, \quad \text{on } S_\mathrm{N} \tag{2c}$$

where L is the Laplacian, V_p the volume of the catalytic body, S_p its external surface (accessible to reactants), S_N is a sealed (inaccessible to reactants) portion of the V_p boundary [Remark: symbol V_p will stand for both, the spatial domain corresponding to the catalyst and its volume; similarly, S_p stands for the domain of the permeable external surface and for its area],

$$\lambda^2 = \frac{J_A}{\pi_{A\mathrm{S}}}; \quad \lambda : \text{global reaction scale} \tag{2d}$$

and the activity a, a function of the spatial coordinate vector $\mathbf{x} = (x_1, x_2, x_3)$, is assumed to be normalized according to:

$$\frac{1}{V_p}\int_{V_p} a(\mathbf{x})\,\mathrm{d}V = 1 \tag{2e}$$

It is assumed that the activity at any point on the external surface is finite, but not necessarily uniform.

3. Asymptotic behaviour at high reaction rates

The local reaction scale at the surface is defined as $\lambda_S = \lambda/a_S^{1/2}$, where a_S is the local value of a at the external pellet surface. When λ_S is small enough, species A will penetrate only a short distance from the external surface before reaching nearly equilibrium conditions (i.e., $Y \approx 0$). It is well known that the local flux can be approximated by $N_{AS,0} = J_A\alpha_1/\lambda_S$ (see e.g. [1]), where α_1 just depends on the form of $r(Y)$. At these conditions, hereinafter called limiting regime, the order of magnitude of the penetration depth is λ_S.

The results for geometries with a high degree of symmetry (e.g., a sphere, a long circular cylinder, and a slab) indicate that at somewhat larger values of λ_S, an expansion of the following type holds up,

$$N_{AS} = \frac{J_A}{\lambda_S}[\alpha_1 + \alpha_2\lambda_S + o(\lambda_S)] \tag{3a}$$

where, in general, $o(x)$ denotes a truncation term such that $[o(x)/x] \to 0$ if $x \to 0$, the coefficient α_2 depends on the form of $r(Y)$, but also on the pellet shape and on the activity gradient at the surface [7,8]. Conditions at which $o(\lambda_S)$ can be neglected in Eq. (3a), but $(\alpha_2\lambda_S)$ cannot, will be referred to as asymptotic regime and the corresponding flux denoted $N_{AS,\mathrm{high}}$. We will present a formulation for α_2 and for the integral of $N_{AS,\mathrm{high}}$ over S_p,

$$R_{\mathrm{high}} = \int_{S_p} N_{AS,\mathrm{high}}\,\mathrm{d}S \tag{3b}$$

The task of developing Eq. (3b) is restricted in this paper to catalysts with smooth external surfaces showing continuous curvatures. We will come back to the latter restriction in Section 4.

3.1. Expressing the Laplacian L(Y)

To formulate the conservation balances in the asymptotic regime, it is convenient to define a system of orthogonal curvilinear coordinates in which one of them, ξ_n, keeps the direction of the normal at any point on S_p, where its origin ($\xi_n = 0$) is defined. Furthermore, the sense and scale of ξ_n are fixed by stating that it grows towards the inside of the pellet while measuring at each point the distance from S_p. With this definition, the Cartesian vector $\mathbf{x} = (x_1, x_2, x_3)$ defining the position of a point inside the catalyst, but sufficiently close to S_p, can be expressed as:

$$\mathbf{x} = \mathbf{x}_S(\xi_1, \xi_2) + \xi_n\mathbf{n}(\xi_1, \xi_2) \tag{4a}$$

where $\mathbf{x}_S(\xi_1, \xi_2)$ is the Cartesian vector describing the position on S_p in terms of coordinates (ξ_1, ξ_2) and $\mathbf{n}(\xi_1, \xi_2)$ is the unit vector ($|\mathbf{n}| = 1$) normal to S_p at the same position, which is oriented towards the inside of the pellet. The new set of curvilinear coordinates (ξ_n, ξ_1, ξ_2) is defined by transformation (4a). The coordinate ξ_n has been completely defined, but (ξ_1, ξ_2) still have to be identified in order that the coordinate system may be orthogonal. We will analyse this feature next, while the feasibility of transformation (4a) will be considered after.

The orthogonality condition requires that the internal product $(\partial\mathbf{x}/\partial\xi_i)\cdot(\partial\mathbf{x}/\partial\xi_j) = 0$, if $i \neq j$. Applied to $(i, j) = (1, n)$, the product becomes $[(\partial\mathbf{x}_S/\partial\xi_1) + \xi_n(\partial\mathbf{n}/\partial\xi_1)]\cdot\mathbf{n}(\xi_1, \xi_2)$, that always will be zero because both vectors $(\partial\mathbf{x}_S/\partial\xi_1)$ and $(\partial\mathbf{n}/\partial\xi_1)$, lie on the surface (see e.g. [9]) and, hence, they are normal to $\mathbf{n}$. The same applies for $(i, j) = (2, n)$. The remaining condition is that for $(i, j) = (1, 2)$,

$$\frac{\partial\mathbf{x}}{\partial\xi_1}\cdot\frac{\partial\mathbf{x}}{\partial\xi_2} = \left(\frac{\partial\mathbf{x}_S}{\partial\xi_1} + \xi_n\frac{\partial\mathbf{n}}{\partial\xi_1}\right)\cdot\left(\frac{\partial\mathbf{x}_S}{\partial\xi_2} + \xi_n\frac{\partial\mathbf{n}}{\partial\xi_2}\right) = 0 \tag{4b}$$

Making $\xi_n = 0$, we conclude that the directions of ξ_1, ξ_2 on the external surface should be orthogonal in order that $(\partial\mathbf{x}_S/\partial\xi_1)(\partial\mathbf{x}_S/\partial\xi_2) = 0$. It is further needed that for $\xi_n > 0$

$$\frac{\partial\mathbf{x}_S}{\partial\xi_1}\cdot\frac{\partial\mathbf{n}}{\partial\xi_2} + \frac{\partial\mathbf{x}_S}{\partial\xi_2}\cdot\frac{\partial\mathbf{n}}{\partial\xi_1} = 0 \tag{4c}$$

Except when S_p is a plane or a sphere, the theory of surfaces (see e.g. [9], p. 139) reveals that Eq. (4c) holds if and only if both families of curves on S_p, defined by $\xi_1 \equiv$ const. and $\xi_2 \equiv$ const., coincide with the lines of curvature. A line of curvature is a curve on a surface such that at any point its direction corresponds to the direction of a principal curvature.[2] One set of curves corresponds to the minimal normal curvature and the other to the maximal one. Both sets are mutually orthogonal and unique for a given surface. Then, we are constrained to choose a pair of curvilinear coordinates, denoted ξ_a and ξ_b, each one parameterizing each set of lines of curvature. For ξ_a and ξ_b, the relations $\partial\mathbf{n}/\partial\xi_i = -\kappa_i\partial\mathbf{x}_S/\partial\xi_i$ (i = a, b) hold [9], where κ_i is the principal curvature in the direction of ξ_i. Then, the set of coordinates (ξ_n, ξ_a, ξ_b) will be orthogonal.

In case of a plane or a spherical surface the concept of lines of curvature looses its meaning (as the value of the normal curvature is independent of direction), but any pair of orthogonal coordinates satisfies $\partial\mathbf{n}/\partial\xi_i = -\kappa\partial\mathbf{x}_S/\partial\xi_i$ (κ is the unique value of normal curvature). We will continue the

[2] For a point P on a surface, assume the normal unit vector $\mathbf{n}$ is identified. Then, a normal plane at P is any plane containing $\mathbf{n}$ (there is a bundle of such planes), a normal section at P is a curve resulting from intersecting the surface and a normal plane, a normal curvature is the curvature of a normal section at P, a principal curvature is either the minimum or the maximum normal curvature, a radius of curvature is the inverse of a normal curvature.

present discussion with the general case in mind, but the formulation will remain valid for a plane or a spherical surface by replacing (ξ_a, ξ_b) by any orthogonal pair (ξ_1, ξ_2).

The scale factors $h_i = |\partial \mathbf{x}/\partial \xi_i|$ of the coordinates are defined by expressing the elementary arc length in the direction of each ξ_i: $ds_i = |\partial \mathbf{x}/\partial \xi_i|\, d\xi_i$. From Eq. (4a), with ($\xi_1$, ξ_2) ≡ (ξ_a, ξ_b):

$$h_i = h_{S,i}(1 - \xi_n \kappa_i), \quad i = \text{a, b}; \qquad h_n = 1 \tag{5a}$$

where $h_{S,i} = |\partial \mathbf{x}_S/\partial \xi_i|$ (i = a, b) are the scale factors on S_p, which depend on the position defined by (ξ_a, ξ_b).

Since a sense for the unit vector **n** has been chosen, the sign of κ_i (i = a, b) becomes defined as positive if the centre of curvature is oriented towards the inside of the pellet and negative in the opposite case.

Eqs. (5a) allow to visualize that the chosen coordinate system will become unfeasible when any of the h_i (i = a, b) becomes nil. As we are interested in positive values of ξ_n, the coordinate system will be feasible only up to some distance from S_p if at least one of the κ_i (i = a, b) is positive. If both are positive, the system becomes unfeasible at $\xi_{n,\max}$:

$$(\text{for } \kappa_i \geq 0, \quad i = \text{a, b}), \quad \xi_{n,\max} = \min_{\text{a,b}}(R_i) \tag{5b}$$

where $R_i = 1/\kappa_i$ (i = a, b) are the principal radii of curvature.

For general orthogonal curvilinear coordinates (ξ_1, ξ_2, ξ_3), the Laplacian of a field Y can be written as:

$$L(Y) = \sum_{k=1}^{3} \frac{1}{H} \frac{\partial}{\partial \xi_k} \left(\frac{H}{h_k^2} \frac{\partial Y}{\partial \xi_k} \right); \quad H = h_1 h_2 h_3 \tag{6a}$$

Taking now our specific system (ξ_n, ξ_a, ξ_b) and the fact that $h_n = 1$ (Eq. (5a)),

$$L(Y) = L_n(Y) + L_{SF}(Y) \tag{6b}$$

where

$$L_n(Y) = \frac{1}{h_a h_b} \frac{\partial}{\partial \xi_n} \left(h_a h_b \frac{\partial Y}{\partial \xi_n} \right) \tag{6c}$$

$$L_{SF}(Y) = \frac{1}{h_b} \frac{\partial}{\partial s_a} \left(h_b \frac{\partial Y}{\partial s_a} \right) + \frac{1}{h_a} \frac{\partial}{\partial s_b} \left(h_a \frac{\partial Y}{\partial s_b} \right) \tag{6d}$$

The notation $\partial s_i = h_i \partial \xi_i$ (i = a, b) is employed in Eq. (6d). The derivative $\partial Y/\partial s_i$ is called physical derivative. It expresses the variation of Y over an elementary arc of length $h_i \partial \xi_i$.

$L_{SF}(Y)$ is the Laplacian of Y on the internal surfaces defined in Eq. (4a) by ξ_n = const., that are parallel to S_p. Eq. (6d), specifically expresses L_{SF} in terms of coordinates (ξ_a, ξ_b).

The following steps are devoted to removing the explicit occurrence of the scale factors h_a and h_b in Eqs. (6c) and (6d) and introducing curvature properties of S_p. First, Eqs. (6c) and (6d) are re-written as:

$$L_n(Y) = \frac{\partial^2 Y}{\partial \xi_n^2} - \Upsilon_n \frac{\partial Y}{\partial \xi_n} \tag{7a}$$

$$L_{SF}(Y) = \sum_{i=\text{a,b}} \left[\frac{\partial}{\partial s_i} \left(\frac{\partial Y}{\partial s_i} \right) - \Upsilon_i \frac{\partial Y}{\partial s_i} \right] \tag{7b}$$

where

$$\Upsilon_n = -\frac{\partial \ln(h_a h_b)}{\partial \xi_n}; \qquad \Upsilon_a = -\frac{\partial \ln(h_b)}{\partial s_a};$$

$$\Upsilon_b = -\frac{\partial \ln(h_a)}{\partial s_b}$$

The quantity Υ_n can be directly evaluated by using Eq. (5a) for h_a and h_b,

$$\Upsilon_n = \frac{\kappa_a}{1 - \xi_n \kappa_a} + \frac{\kappa_b}{1 - \xi_n \kappa_b} \tag{8}$$

We again employ Eq. (5a) for expressing Υ_a and Υ_b. For (i, j) = (a, b) or (i, j) = (b, a):

$$\Upsilon_j = \frac{-1}{h_i} \left(\frac{\partial h_{S,i}}{h_j \partial \xi_j}(1 - \xi_n \kappa_i) - h_{S,i} \xi_n \frac{\partial \kappa_i}{h_j \partial \xi_j} \right)$$

$$= \frac{-1}{(1 - \xi_n \kappa_j)} \left(\frac{\partial \ln h_{S,i}}{h_{S,j} \partial \xi_j} - \frac{\xi_n}{(1 - \xi_n \kappa_i)} \frac{\partial \kappa_i}{h_{S,j} \partial \xi_j} \right) \tag{9a}$$

which requires the evaluation of $\partial h_{S,i}/\partial \xi_j$ and $\partial \kappa_i/\partial \xi_j$ ($i \neq j$). To this end, the following formulation is used:

$$(i \neq j): \quad \frac{\partial \ln h_{S,i}}{h_{S,j} \partial \xi_j} = -\kappa_{g,i} \tag{9b}$$

$$\frac{\partial \kappa_i}{h_{S,j} \partial \xi_j} = \kappa_{g,i}(\kappa_i - \kappa_j) \tag{9c}$$

Eq. (9b) arises from the definition of geodesic curvature $\kappa_{g,i}$ for any pair of orthogonal coordinates [Remark: at a given point on the surface, $\kappa_{g,i}$ is the curvature of the projection of the coordinate curve ξ_i on the tangent plane]. If the curvature of the own coordinate line is $\kappa_{\xi,i}$, then at the given point: $\kappa_i^2 + \kappa_{g,i}^2 = \kappa_{\xi,i}^2$. Eq. (9c) arises from the formulae of Mainardi–Codazzi [9] and is valid when the coordinate curves are lines of curvature, and in the case of a spherical or plane surface for any pair of orthogonal coordinates. Replacing Eqs. (9b) and (9c) into Eq. (9a), the following expressions arise:

$$\Upsilon_a = \frac{\kappa_{g,b}}{1 - \xi_n \kappa_b} \tag{9d}$$

$$\Upsilon_b = \frac{\kappa_{g,a}}{1 - \xi_n \kappa_a} \tag{9e}$$

With Eqs. (8), (9d) and (9e), the Laplacian $L(Y)$ (Eq. (6b)) becomes fully expressed in terms of curvature properties of S_p. In turn, the conservation balance in Eq. (2a) becomes:

$$\frac{\partial^2 Y}{\partial \xi_n^2} - \Upsilon_n \frac{\partial Y}{\partial \xi_n} + \sum_{i=\text{a,b}} \left[\frac{\partial}{\partial s_i} \left(\frac{\partial Y}{\partial s_i} \right) - \Upsilon_i \frac{\partial Y}{\partial s_i} \right]$$

$$= \frac{1}{\lambda^2} a(\xi_n, \xi_a, \xi_b) r(Y) \tag{10}$$

3.2. Reduction of Eq. (10) at low values of λ

Let us introduce in Eq. (10):

- $a^* = a(\xi_n, \xi_a, \xi_b)/a_S$: relative activity, where $a_S = a(0, \xi_a, \xi_b)$.
- $\lambda_S = \lambda/a_S^{1/2}$: local reaction scale on S_p,
- $\zeta = \xi_n/\lambda_S$: stretched coordinate.

Then,

$$\frac{\partial^2 Y}{\partial \zeta^2} - \lambda_S \Upsilon_n \frac{\partial Y}{\partial \zeta} + \lambda_S^2 L_{SF}(Y) = a^*(\xi_n, \xi_a, \xi_b) r(Y) \tag{11a}$$

Assuming that λ_S is small enough for the penetration depth to be shorter than the thickness d of the pellet in the local normal direction, i.e.

$$\lambda_S \ll d \tag{11b}$$

the appropriate boundary conditions on variable ζ will be:

$$\zeta = 0: \quad Y = 1 \tag{11c}$$

$$\zeta \to \infty: \quad Y \to 0, \quad \left(\frac{\partial Y}{\partial \zeta}\right) \to 0 \tag{11d}$$

Now, consider the following simplified problem,

$$\frac{d^2 Y_0}{d\zeta^2} = r(Y_0) \tag{12a}$$

$$\zeta = 0: \quad Y_0 = 1 \tag{12b}$$

$$\zeta \to \infty: \quad Y_0 \to 0, \quad \left(\frac{dY_0}{d\zeta}\right) \to 0 \tag{12c}$$

that corresponds to the limiting regime previously defined. The solution of Eqs. (12) is well known (see e.g. [1] and also Appendix B) and can be expressed by:

$$\frac{dY_0}{d\zeta} = -I(Y_0)^{1/2} \tag{12d}$$

where

$$I(Y_0) = 2\int_0^{Y_0} r(Y)\, dY \tag{12e}$$

In particular, the flux on the external surface S_p ($\zeta = 0$):

$$N_{AS,0} = -\frac{J_A}{\lambda_S}\left(\frac{dY_0}{d\zeta}\right)_{\zeta=0} = \frac{J_A}{\lambda_S} I_1 \tag{13a}$$

$$I_1 = [I(1)]^{1/2} \tag{13b}$$

The following points are worth noting:

(I) Conditions $Y_0 \to 0$ $(dY_0/d\zeta) \to 0$ in Eq. (12c) are already satisfied, for practical purposes, when ζ reaches a few units.

(II) Y_0, $r(Y_0)$ and the derivatives $(\partial Y_0/\partial\zeta)$ and $(\partial^2 Y_0/\partial\zeta^2)$ show maximum absolute values around the unity.

For Eq. (12a) to approximate Eq. (11a) it is necessary that $|\lambda_S \Upsilon_n| \ll 1$, $|\lambda_S^2 L_{SF}(Y)| \ll 1$, and $a^* \approx 1$. These conditions will be fulfilled for a sufficiently small value of λ_S. In what follows, practical scales respect to which λ_S should be small in order to guarantee those conditions will be determined. At the same time, the terms of second order of magnitude linking Eqs. (12a) and (11a) will be identified. This task will allow us to write down a conservation balance describing the asymptotic regime. In the next paragraphs, it should be borne in mind that the solution Y of the asymptotic regime will keep the same order of magnitude as Y_0. Then, points (I) and (II) stated above will hold up in the asymptotic regime by exchanging Y_0 for Y.

3.2.1. Analysis of $\lambda_S \Upsilon_n$

From Eq. (8) a series expansion of Υ_n about $\xi_n = 0$ can be written (using $\xi_n = \zeta\lambda_S$)

$$\Upsilon_n = \Upsilon_S + \sum_{j=1}^{\infty} (\kappa_a^{j+1} + \kappa_b^{j+1})(\lambda_S \zeta)^j \tag{14a}$$

where $\Upsilon_n|_{\xi_n=0} = \Upsilon_S$, is the sum of the local principal curvatures

$$\Upsilon_S = \kappa_a + \kappa_b = \frac{1}{R_a} + \frac{1}{R_b} \tag{14b}$$

[Remark: the quantity $\Upsilon_S/2$ is known as mean curvature]

We are looking for conditions at which $|\lambda_S \Upsilon_n| \ll 1$. From the leading term in expansion (14a), it becomes apparent that a necessary condition is that $|\lambda_S \Upsilon_S| \ll 1$. If we define

$$R_m = \min\{|R_a|, |R_b|\} \tag{14c}$$

an equivalent constraint is

$$\lambda_S \ll R_m \tag{14d}$$

In addition, if Eq. (14d) is fulfilled, we can write from Eq. (14a) for small values of ζ (i.e., up to a few units),

$$\lambda_S \Upsilon_n = \lambda_S \Upsilon_S + \zeta O\left[\left(\frac{\lambda_S}{R_m}\right)^2\right] \tag{14e}$$

[Remark: the symbol $O(x)$ is used throughout this text and its appendices to denote a variable that takes values "of the same order of magnitude as x"].

It is also worth noting at this point that condition (14d) insures that Eq. (5b), which restrains the range of feasibility of our coordinate system, will not be violated for significant values of ζ (up to a few units).

3.2.2. Analysis of a^*

A series expansion of a^* about $\xi_n = 0$ can be written (after replacing $\xi_n = \zeta\lambda_S$) and dividing by a_S

$$a^* = 1 + \left(\frac{a_S'}{a_S}\right)\lambda_S \zeta + \frac{1}{2}\left(\frac{a_S''}{a_S}\right)(\lambda_S \zeta)^2 + \ldots \tag{15a}$$

where $a_S = a|_{\xi_n=0}$, $a'_S = (\partial a/\partial \xi_n)|_{\xi_n=0}$ and generically $a_S^{(i)} = (\partial^i a/\partial \xi_n^i)|_{\xi_n=0}$. From Eq. (15a), a necessary condition for $a^* \cong 1$ to be true is that:

$$\lambda_S \ll \frac{a_S}{|a'_S|} \tag{15b}$$

If the magnitude of higher order derivatives is bounded as $(1/j!)(a_S^{(j)}/a_S) = O(|a'_S/a_S|^j)$, which will be usually accomplished, the inequality (15b) guarantees that the sequence of terms in Eq. (15a) are of decreasing magnitude for small values of ζ (up to few units). Then, it will be valid to write:

$$a^* = 1 + \left(\frac{a'_S}{a_S}\right)\lambda_S\zeta + \zeta^2 O\left[\left(\frac{\lambda_S a'_S}{a_S}\right)^2\right] \tag{15c}$$

3.2.3. Analysis of $\lambda_S^2 L_{SF}(Y)$

Because of boundary condition (2b), the Laplacian $L_{SF}(Y) = 0$ at S_p ($\xi_n = 0$). Then, by recalling that L_{SF} applies in general ($\xi_n > 0$) over surfaces parallel to S_p, it is difficult to expect that $\lambda_S^2 L_{SF}(Y)$ can contribute significantly in Eq. (11a). Provided that constraints (14d) and (15b) are satisfied and that variations of a_S and curvature radii on S_p are not extreme, it is shown in Appendix A that:

$$\lambda_S^2 L_{SF}(Y) = O\left(\max\left\{\frac{\lambda_S^2}{(a_S/a'_S)^2}, \frac{\lambda_S^2}{R_m|a_S/a'_S|}\right\}\right) \tag{16a}$$

At these conditions, $\lambda_S^2 L_{SF}(Y)$ is correctly neglected for the limiting regime.

For the case of the asymptotic regime, $\lambda_S^2 L_{SF}(Y)$ can also be neglected because only terms of secondary order of magnitudes will be retained in Eq. (11a)

Therefore, taking in Eq. (11a) $\lambda_S \Upsilon_n \approx \lambda_S \Upsilon_S$, $a^* \approx 1 + \zeta\lambda_S(a'_S/a_S)$, and $\lambda_S^2 L_{SF}(Y) \approx 0$ (from Eqs. (14e), (15c) and (16a)), we obtain the desired conservation balance defining the asymptotic regime:

$$\frac{d^2Y}{d\zeta^2} - \lambda_S\Upsilon_S\frac{dY}{d\zeta} = \left[1 + \lambda_S\zeta\left(\frac{a'_S}{a_S}\right)\right] r(Y) \tag{17a}$$

with boundary conditions

$$\zeta = 0; \quad Y = 1 \tag{17b}$$

$$\zeta \to \infty : Y \to 0, \quad \left(\frac{dY}{d\zeta}\right) \to 0; \tag{17c}$$

3.3. Expressing the effective reaction rate in the asymptotic regime

A perturbation analysis on Eqs. (17) considering λ_S as a small parameter can be carried out to obtain the leading terms of the flux at the external surface. The derivation is similar to that made by Wedel and Luss [3], and is detailed in Appendix B. The results is:

$$N_{AS,\text{high}} = -\frac{J_A}{\lambda_S}\left(\frac{dY}{d\zeta}\right)_{\zeta=0} = J_A\left[\frac{I_1}{\lambda}a_S^{1/2} - I_2(\Upsilon_S + A_S)\right] \tag{18}$$

where $\lambda_S = \lambda/a_S^{1/2}$ was used, and

$$I_2 = \frac{1}{I_1}\int_0^1 [I(Y)]^{1/2}\,dY \tag{19a}$$

$$A_S = -\frac{a'_S}{2a_S} \tag{19b}$$

Terms of leading order of magnitude $O(\lambda_S/R_m)$, $O(\lambda_S|a'_S|/a_S)$ have been neglected in Eq. (18). The term $I_2(\Upsilon_S + A_S)$ is a second order correction to the limiting regime expression (13a).

By integrating Eq. (18), the total number of moles transferred per unit time through S_p in the asymptotic regime is:

$$R_{\text{high}} = J_A S_p\left[\frac{I_1}{\lambda}(a_S^{1/2})_{av} - I_2(\Upsilon_S + A_S)_{av}\right]$$

where

$$(a_S^{1/2})_{av} = S_p^{-1}\int_{S_p} a_S^{1/2}\,dS \tag{20a}$$

$$(\Upsilon_S + A_S)_{av} = S_p^{-1}\int_{S_p}(\Upsilon_S + A_S)\,dS \tag{20b}$$

By defining $\mathbb{R} = I_2/I_1$, the characteristic length of the catalyst $\ell = V_p/S_p$, and

$$\Gamma = \frac{\ell(\Upsilon_S + A_S)_{av}}{(a_S^{1/2})_{av}} \tag{21}$$

we can alternatively write for R_{high}

$$R_{\text{high}} = \frac{J_A S_p (a_S^{1/2})_{av} I_1}{\lambda}\left[1 - \mathbb{R}\frac{\lambda}{\ell}\Gamma\right] \tag{22}$$

Employing the usual definition of the effectiveness factor $\eta = R/(\pi_{As}V_p)$ and the Thiele modulus $\Phi^2 = (\ell/\lambda)^2 = \ell^2\pi_{As}/J_A$,

$$\eta_{\text{high}} = \frac{I_1(a_S^{1/2})_{av}}{\Phi}\left(1 - \frac{\mathbb{R}}{\Phi}\Gamma\right) \tag{23}$$

For the case of uniform activity:

$$(a = 1) \quad \eta_{\text{high}} = \frac{I_1}{\Phi}\left(1 - \frac{\mathbb{R}}{\Phi}\Gamma\right); \quad \Gamma = \ell(\Upsilon_S)_{av} \tag{24}$$

4. Discussion

The use of the lines of curvature as coordinates lines, as employed for the derivation of Eqs. (22)–(24), strictly implies

Table 2
Comparison of η for different shapes showing $Q = 0.75$; y: radius ratio; γ: defined in the text; Δ: maximum relative difference

	Infinitely long solid cylinder	Hollow sphere with accessible center, $y = 0.1896$	Hollow sphere with inert core, $y = 0.6300$
Δ (%)	–	0.95	1.2
γ	0.500	0.478	0.470

Table 3
Comparison of η for different shapes showing $Q = 0.50$; y: radius ratio; γ: defined in the text, Δ: maximum relative difference

	Infinitely long hollow cylinder, $y = 0.5773$	Hollow sphere with accessible center, $y = 0.3460$	Hollow sphere with inert core, $y = 0.7937$
Δ (%)	–	0.15	0.30
γ	0.412	0.412	0.407

that S_p should exhibit continuous normal curvatures over its extension. However, this restriction can be relaxed by asking that the continuity condition holds within a number of sections in which the external surface can be divided; hence, admitting curvature jumps between sections.

For example, consider a pellet formed by a circular cylinder of height H and radius R_p and two hemispherical heads of the same diameter at both ends (Fig. 1). This surface is smooth, in the usual sense that the normal vector can be unambiguously defined at each of its points, but across both circles bounding the cylinder and the hemispheres the normal curvature in the direction parallel to the axis presents a jump (between 0 and $1/R_p$). Eqs. (22)–(24) can indeed be straightforwardly applied to this geometry with no further constraints than Eqs. (11b), (14d) and (15b). This seems to contradict the condition for neglecting $L_{SF}(Y)$ (see also Appendix A), requiring that curvatures do not undergo large variations. However, when such variations are confined to curves on S_p (i.e., to a subset of lower dimension), as for the circles in the example, they do not affect the overall validity of Eqs. (22)–(24).

For the catalytic body just considered, $\Upsilon_S = 1/R_p$ on the cylindrical portion and $\Upsilon_S = 2/R_p$ on the spherical caps. Then Γ (Eq. (24)) becomes:

$$\Gamma = \frac{\left(4 + \frac{H}{R_p}\right)\left(4 + \frac{3H}{R_p}\right)}{6\left(2 + \frac{H}{R_p}\right)^2} \tag{25}$$

Taking $H = 0$ in Eq. (25), we obtain the result $\Gamma = 2/3$ for a sphere, while $H \to \infty$ leads to the value $\Gamma = 1/2$ that holds for an infinitely long circular cylinder.

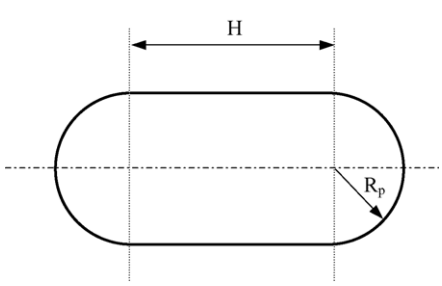

Fig. 1. Sketch of the pellet formed by a circular cylinder and two hemispherical heads.

4.1. The use of Γ as a shape factor

Buffham [10] defined a quantity called compactness to characterize the shape of particles and discussed about its potential use for a variety of technological and scientific applications. In that paper, the use of compactness (here denoted by Q) for the evaluation of effectiveness factor in catalytic pellets with uniform activity was quantitatively assessed. The relation between Q and the parameter Γ at uniform activity (Eq. (24)) is:

$$Q = 1.5\Gamma = \tfrac{3}{2}\ell(\Upsilon_S)_{av} \tag{26}$$

The factor 3/2 renders $Q = 1$ for a sphere. Buffham [10] pointed out different reasons why Q can be suitable to represent the shape of particulate materials in several applications.

In particular, when considering different geometries representing smooth catalytic pellets with the same value of Q, a remarkable similarity was found for the effectiveness factor η of a first order reaction,[3] compared on the basis of the same value of Φ. The two series of results in his paper, for $Q = 0.75$ and 0.5, are summarized in Tables 2 and 3, where γ is a geometric parameter that allows approximating η at low values of Φ [1,5]. In particular, for a first order reaction, $\eta \approx 1 - \gamma\Phi^2$.

As pointed out by Buffham [10], the hollow sphere with accessible center cannot be related to a real catalyst pellet, but it provides a simple geometric alternative. The results in Tables 2 and 3 suggest that Q (hence, Γ) can be an excellent correlator for the shape of catalyst pellets. Other examples, including cylindrical pellets of finite length and different cross sections can be included, but this requires adding the effect of edges. These results will be presented in a separate contribution.

Nonetheless, counter-examples arise when considering washcoats in monolithic reactors. In Table 4, monoliths with circular cross-section and square cross-section channels are considered. The washcoat will be naturally circular in circular channels, but the washcoat tends to grow thicker at the corners of square channels. The case considered in Table 4

[3] When invoking "first order reaction", it is assumed that $r_A = kC_A$, isothermal system and that $N_A = -D_A \nabla C_A$, with constant D_A; hence, $Y = C_A/C_{AS}$, $r(Y) = Y$.

Table 4
Comparison of η for different shapes showing $Q = 0.285$ ($\Gamma = -0.19$); $y = a/b$; γ: defined in the text; Δ: maximum relative difference

Catalyst	Cross-section	Dimensions	γ	Δ (%)
Monolith channel square cross-section (SCS)	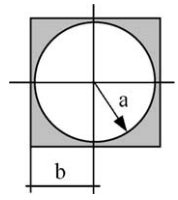	$y = 0.96$	0.779	–
Four-hole-cylinder accessible from inner and outer surfaces	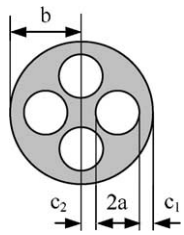	$y = 0.306$, $c_1 = 0.634$ a, $c_2 = 0.634$ a	0.419	16.5 ($\Phi = 1.42$)
Monolith channel circular cross-section (CCS)	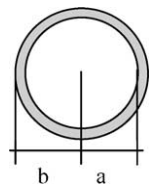	$y = 0.851$	0.306	23.8 ($\Phi = 1.42$)

is one of the four examples analised by Papadias et al. [2]. The third geometry is that of a four-hole-cylinder (accessible from the outer and inner perimeters), and it closely corresponds to the shape of a commercial pellet, although it is here assumed as being infinitely long. The three geometries present $Q = -0.285$ ($\Gamma = -0.19$). The negative compactness is a feature of washcoat geometries. Now, the effectiveness factors of a first order reaction show large discrepancies among the three shapes. The reason for this behaviour is that the three geometries show considerable different values of the parameter γ. In particular, a very high value of γ arises for the washcoat in the square cross-section channel.

These results indicate that Q, or Γ, does not always suffice to characterize quantitatively the behaviour of a catalytic body. As parameters Γ and γ control the behaviour at high and low reaction rates respectively, it seems to be necessary that both should match (at least in an approximate sense) for different shapes to show the same behaviour. This happens in the examples of Tables 2 and 3, but it does not hold in Table 4.

We should emphasize at this point that the importance of being capable of characterizing geometrically a catalytic body is that simple geometries can be employed to predict the behaviour of geometrically complex catalytic bodies. For example, both the infinitely long four-hole-cylinder and the washcoat in the square cross-section channel are 2D bodies; so it would be desirable to find a 1D body with an equivalent shape and use it as a geometric model. For this case, the hollow cylinder could have been such a model, but the result shows that it can only provides a rough approximation for the four-hole-cylinder.

The parameter Γ is just a geometric parameter when the activity is uniform, Eq. (24), and it is composed of a geometric term plus an activity dependent coefficient when the activity is not uniform (Eq. (21)). Thus, in general, a given catalytic body should have to be characterized, as far as the high reaction rate behaviour is concerned, by the combined effects expressed in the definition of Γ in Eq. (21).

It is important to stress that the parameter Γ occurs in the second order correction term of Eq. (23) as a factor separable from the factor $\mathbb{R}$ that depends on kinetic parameters. Actually, this property allows the chance of characterizing a catalytic body by its value of Γ, independently of kinetics. It is also worth recalling that $\mathbb{R} = I_2/I_1$ not only depends on kinetic parameters, but on transport coefficients and on the state variables at S_p (except in some elementary cases).

4.2. *The use of Eq. (23) to complement numerical calculations*

Irrespective of the use of Γ as a shape parameter, Eq. (23) can be directly employed to evaluate η provided that the appropriate conditions for its use have been reached. In particular, for a precise evaluation of η, a numerical solution of the 2D or 3D conservation equations can be performed when Φ is relatively low and Eq. (23) can be used when Φ is high, a strategy that will avoid the very high numerical cost

demanded at high values of Φ. For this application, it is important to recall the main constraints for Eq. (23) (as expressed in Eqs. (11b), (14d) and (15b)) that, in principle, should be satisfied at each point on S_p. Because $\lambda = \ell/\Phi$, these constraints impose a lower limit on the values of Φ. The minimum value Φ_m at which Eq. (23) can be employed varies, mainly with the geometry. For a first order reaction and uniform activity, $\Phi_m \approx 1$ for a sphere and $\Phi_m \approx 6$ for the washcoat on the square channel considered in Table 4. According to our calculations still in progress, these examples provide extreme values of Φ_m; more typical and frequent values are $\Phi_m \in [2, 2.5]$. In any case, the magnitude of the second order correction ($\mathbb{R}\Gamma/\Phi$) in Eq. (23) can reach in practice up to about 30%.

4.3. The effect of external transport limitations

It is important to consider the influence that external transport limitations can exert on the assumption about uniform state variables on S_p (assumption (a) in Section 2). We first note that Eq. (18) for the local flux $N_{AS,high}$ will be still valid if the state variables are not uniform (except for extreme gradients over S_p). Hence, the local composition can be evaluated from local conservation balances for each generic species j:

$$\left(\frac{\nu_j}{\nu_A}\right) N_{AS,high} = k_{mj}(C_{jF} - C_{jS}) \tag{27a}$$

where C_{jF} is the average concentration in the fluid phase and k_{mj} is the local mass transfer coefficient for j [Remark: more general expressions for the external flux will not alter the significance of the present discussion; also, an expression analogous to Eq. (27a) can be used for temperature]. Expressing in Eq. (27a) $N_{AS,high}$ from Eq. (18)

$$[\{C_{jS}\}: \text{ variable on } S_p] \quad \left(\frac{\nu_j}{\nu_A}\right) J_A \times \left[a_S^{1/2}\frac{I_1}{\lambda} - I_2(\Upsilon_S + A_S)\right] = k_{mj}(C_{jF} - C_{jS}) \tag{27b}$$

If at least one quantity of the set $\{a_S, A_S, \Upsilon_S, k_{mj}\}$ changes over S_p, the local composition $\{C_{jS}\}$ will vary over S_p. In any case, after solving Eq. (27b) for $\{C_{jS}\}$ (considering the dependence of J_A, I_1, I_2 and λ), $N_{AS,high}$ can be integrated over S_p to obtain R_{high}. If this is our final purpose, the usefulness of Eq. (18) for $N_{AS,high}$ is evident.

However, if $\{C_{jS}\}$ turns out to be non-uniform, this procedure prevents R_{high} from being written in terms of the parameter Γ, and its meaning as a relevant shape factor will become obscure without further analysis. With this purpose in mind, let us assume that uniform values $\{C_{jS}\}$ apply on an approximate basis. Then, instead of Eq. (27a) we can use the overall expression:

$$\left(\frac{\nu_j}{\nu_A}\right) R_{high} = K_j(C_{jF} - C_{jS}) \tag{28a}$$

where $K_j = \int_{S_p} k_{mj}\,dS$, and R_{high} is expressed by Eq. (22). Then

$$[\{C_{jS}\}: \text{ uniform on } S_p] \quad \left(\frac{\nu_j}{\nu_A}\right) \frac{J_A(a_S^{1/2})_{av} I_1}{\lambda} \times \left[1 - \mathbb{R}\frac{\lambda}{\ell}\Gamma\right] = \left(\frac{K_j}{S_p}\right)(C_{jF} - C_{jS}) \tag{28b}$$

Eq. (28b) involves an overall set $\{C_{jS}\}$ that represents uniform state variables over S_p.

In general, differences between values of R_{high} using either local values of $\{C_{jS}\}$(i.e., from of Eq. (27b)) or an overall set $\{C_{jS}\}$from (28b) will depend on the extend of variations of the quantities $\{a_S, A_S, \Upsilon_S, k_{mj}\}$ over S_p, but also on the average impact of the external limitations. For example, if we tolerate differences less than 2%, calculations for a first order reaction show that if the net effect of external limitations on R_{high} is not higher than around 10%, values of k_m (uniformly distributed over S_p) can vary up to six-fold. On the other hand, if k_m varies in less than around 2.5-fold, the net external transport effect can be of any strength and Eq. (28b) will still be accurate.

In practice, k_m can effectively undergo strong changes over S_p (a brief discussion in this regard is given below) that will directly influence the results from Eq. (27b), but variables of the catalyst side, a_S, A_S, Υ_S, are not likely to cause a similar influence. In fact, expressions (14d) and (15b) restrain the effect of A_S and Υ_S in the left-hand side of Eq. (27b) to 20–30%, and a_S will be usually almost uniform. Hence, we can conclude that the left-hand side of Eq. (27b) will be not a significant source for non-uniform values of $\{C_{jS}\}$. Therefore, instead of taking local values of a_S, A_S and Υ_S in Eq. (27b), it will be still accurate to take their averages over S_p. Thus, the approximate, but accurate, local condition suggested to replace Eq. (27b) is:

$$[\{C_{jS}\}: \text{ variable on } S_p] \quad \left(\frac{\nu_j}{\nu_A}\right) \frac{J_A I_1 (a_S^{1/2})_{av}}{\lambda} \times \left[1 - \mathbb{R}\frac{\lambda}{\ell}\Gamma\right] = k_{mj}(C_{jF} - C_{jS}) \tag{29}$$

which shows that the meaning of Γ will be preserved, even when $\{C_{jS}\}$ varies on S_p.

It seems appropriate at this point to consider briefly the actual magnitude of external transport limitations, at least in the case of one-phase flow. In monolithic reactors, the usual laminar regime and large ratios of channel to catalytic cross-section areas increase the relative impact of external limitations, i.e., the asymptotic regime will be reached along with significant external effects. This can be checked by taking realistic values of geometric and transport properties in both, the channels and the washcoat. For the non-circular channels studied by Hayes et al. [11], k_m evidenced significant intrinsic variations around the perimeter. Nonetheless, except in some instances of very strong external limita-

tions (i.e., very low values of C_{AS}/C_{AF}) changes of C_{AS} around the perimeter were not larger than ±30% of the average.

On the other hand, the impact of external limitations is expected to be weaker in packed beds, since inertial or turbulent flow regimes prevail and ratios of catalyst to interstitial volumes are large. Hence, it will be usual to find practical cases combining the asymptotic regime and negligible external limitations, although counterexamples cannot be ruled out. Local variations of k_m around the particle take place primarily due to boundary layer effects that in turn depend on the influence of neighbouring particles (contact points) and on the shape of the particle. For example, Gillespie et al. [12], measured heat transfer coefficients that varied by a factor of 2–4 around a test sphere in a randomly packed bed. As expected, the distribution of k_m notoriously changed with the specific location of the test sphere in the bed.

We can conclude that the effect of external transport limitations cannot be ignored for fast reaction conditions as those leading to the asymptotic regime, but instances of significant local effects will be scarce. In any case, it is most probable that the role of Γ as a significant shape parameter will hold up.

4.4. Extension to multiple reactions

So far, we have dealt with a single reaction. If a simple 1D model is desirable for avoiding 2D or 3D calculations when a single reaction takes place, much more significant will be the possibility of such approximation for multiple reaction systems. In principle, we should ask if Γ, just as defined in Eq. (21), is also useful for characterizing such type of systems.

Fortunately, the answer is affirmative, as shown in Appendix C. It is shown there that when the whole reacting system is in the asymptotic regime, the second order correction for all the effective reaction rates will depend on the same parameter Γ (see Eq. C17). The coefficients that play the role of I_1 and I_2 will be no longer available in a close way, but the rate R_{high} can be calculated from a single 1D numerical evaluation, as explained in Appendix C.

The above discussion on the effect of external transport limitations remains valid for multiple reactions, and expressions similar to Eqs. (27)–(29) can be written from the formulation given in Appendix C.

Assumption (b) in Section 2, concerning the transport model inside the catalyst, deserves a final comment. It is shown in Appendix C for the general case of multiple reactions that 1D conservation equations and local flux expressions for the asymptotic regime (i.e., Eqs. (17a) and (18) for a single reaction and Eqs. (C9) and (C16) of Appendix C for the general case) can be written without the need of imposing assumption (b). Instead, a closed equation for R_{high} (e.g., as in Eq. (22)) is not already possible, due to the local dependence of transport parameters.

5. Conclusions

The main results of this paper are Eqs. (21)–(24) expressing the effective reaction rate in terms of $(1/\Phi)$ and $(1/\Phi)^2$ for smooth 2D or 3D catalyst shapes. Conditions at which these expressions apply are termed asymptotic regime. Eqs. (21)–(24) have been developed from the choice of a proper curvilinear coordinate system that facilitates introducing the condition of small penetration depth to approximate the conservation equation by a unidirectional form (Eqs. (17)).

Significant restrictions for such approximation can be expressed in terms of activity gradients at the external surface S_p (Eq. (15b)), curvature properties of S_p (Eq. (14d)) and the depth of the catalyst measured from S_p (Eq. (11b)).

Parameter Γ (Eq. (21)) defines the magnitude of the second order correction and depends on the integral over S_p of the average curvature and of the activity gradient. Based on qualitative arguments and for uniform activity, Buffham [10] proposed a quantity proportional to Γ as a general shape factor for granular materials and provided a number of examples showing that the effectiveness factor for different geometries with the same value of Γ were very much the same at any value of Φ. The expressions for the asymptotic regime confirm that such parity among different geometries at least requires that Γ be nearly the same, but it has been shown here that the behaviour at low reaction rates, characterized by a different shape factor (γ) should also match. The importance of defining suitable shape factors stems in the possibility of finding 1D geometric simplifications for complex catalyst shapes. The parameter Γ will be crucial to that end, and a systematic study is being presently carried out. The current investigation includes extending the analysis of the asymptotic regime for catalyst shapes showing edges. In essence, this involves introducing an additional term to the expressions here developed.

Another important use of the expressions for the asymptotic regime is for complementing a numerical evaluation of the conservation equation: a numerical method can be employed for the relatively smooth concentration fields at low values of Φ, while the asymptotic expression can be used at large Φ, when steep (and difficult to evaluate) solutions take place.

Although most of the material in this paper is discussed on the basis of a single reaction, it has been shown in Appendix C that the main conclusions hold for multiple reactions, if all of them have reached the asymptotic regime: the significance of parameter Γ is maintained and an equivalent formulation applies. A general form of conservation equations (1D differential equations holding on a local basis over S_p) for the asymptotic regime, without assuming uniform state variables on S_p and for an arbitrary transport model inside the catalyst, is also presented in Appendix C.

Acknowledgements

The authors wish to thank the financial support of the following Argentine institutions: ANPCyT- SECyT (PICT N# 14224) and UNLP (PID N# 11/I078). N.J.M., O.M.M. and G.F.B. are research members of the Conicet and S.D.K. is a fellow of the Academia Nacional de Ciencias Exactas, Físicas y Naturales.

Appendix A

A.1. Order of magnitude estimate of $\lambda_S^2 L_{SF}(Y)$

In this appendix, we will undertake the evaluation of the magnitude of $\lambda_S^2 L_{SF}(Y)$ in Eq. (11a) at low values of λ. To this end, the concept of scale of variation will be useful. The scale of variation of a quantity Q in the direction of coordinate i, $\Delta_{Q,i}$ (≥ 0), is such that it allows an order of magnitude estimate of the physical derivative, according to $O(\partial Q/\partial s_i) = Q/\Delta_{Q,i}$.

Consider first equation (9c) for estimating the order of magnitude of the geodesic curvatures $\kappa_{g,i}$. We can rewrite the left-hand side of Eq. (9c) as:

$$\frac{\partial \kappa_i}{h_{S,j}\partial \xi_j} = \frac{-1}{R_i^2}\frac{\partial R_i}{h_{S,j}\partial \xi_j}$$

We will assume that the scale of variation of the radius of curvature R_i will not be shorter than $|R_i|$. Cases not satisfying this condition will be hard to find in catalytic bodies.

Taking $\Delta_{R_{i,j}} \sim |R_i|$ (i = a, b; j = a, b), we obtain an (usually) upper estimate of $|\kappa_{g,i}|$ from Eq. (9c): $|\kappa_{g,i}| = O[\kappa_i^2/(\kappa_a - \kappa_b)]$. Assuming that κ_a and κ_b are not very close to each other, we can simplify this estimation by writing $|\kappa_{g,i}| = O(1/R_m)$, where $R_m = \min\{|R_a|, |R_b|\}$ (Eq. (14c) of the main text).

The estimate $|\kappa_{g,i}| = O(1/R_m)$, for i = a, b, will not longer hold around an umbilic point of the surface. An umbilic point is an isolate point on the surface at which $\kappa_a = \kappa_b$ (equivalently, $R_a = R_b$), and it is a singular point for the specific coordinates (ξ_a, ξ_b): along any direction on the surface leading to an umbilic point, $\kappa_a \to \kappa_b$ and for the coordinate curves, $h_{S,i} \to 0$, $\kappa_{g,i} \to \infty$ (i = a or b). As a result, some of the terms in L_{SF} (Eq. (7b)) become individually undetermined, but when L_{SF} is properly handled as a whole, a regular value arises for it. This is so because the Laplacian L_{SF} is an invariant (zero order tensor), and as such can be evaluated from any suitable pair of coordinates (ξ_1, ξ_2), a condition that holds true anywhere, but in particular around the umbilic point.

This can be illustrated by acknowledging that the zone around an umbilic point may be closely represented as a portion of a spherical surface. Employing for this zone any pair of orthogonal coordinates (ξ_1, ξ_2) substituting (ξ_a, ξ_b) in the coordinate system, we will be able to replace Eqs. (9d) and (9e) with $\Upsilon_i = R_p\kappa_{g,i}/(R_p - \xi_n)$, ($i$ = 1, 2), where R_p is the radius of curvature of the spherical surface. Now, $\kappa_{g,i}$ will just depend on the particular choice of (ξ_1, ξ_2). If we take standard spherical coordinates with the equator passing through the umbilic point, it can be shown that $\kappa_{g,i} = 0$ at the umbilic point for both, i = 1, 2. Thus, the only relevant geometric quantity in L_{SF} will be the radius R_p.

With these considerations in mind, we will continue working with the general case $\kappa_a \neq \kappa_b$ and keeping the estimate $|\kappa_{g,i}| = O(1/R_m)$, as the existence of umbilic points does not introduce any essential singularity.

The magnitude of $\lambda_S^2 L_{SF}(Y)$ can be estimated by assuming in a first step that it is negligible and solving the resulting equation (i.e., Eqs. (17) in the main text). From the solution obtained, we should check in a second step if neglecting $\lambda_S^2 L_{SF}(Y)$ was sound.

The type of solutions from Eqs. (17) is analyzed in Appendix B. Eq. (B13) can be written as:

$$Y \approx Y_0(\zeta) + (\lambda_S \Upsilon_S)Y_\Upsilon(\zeta) + \left(\frac{\lambda_S a_S'}{a_S}\right) Y_a(\zeta) \tag{A1}$$

where maximum absolute values of the functions $Y_0(\zeta)$, $Y_\Upsilon(\zeta)$ and $Y_a(\zeta)$ and of their derivatives respect to ζ can be regarded as being around the unity. Recalling that $\zeta = \xi_n/\lambda_S$ and $\lambda_S = \lambda/a_S^{1/2}$, it can be visualized from Eq. (A1) that the dependency of Y on the coordinates ξ_a and ξ_b will arise throughout the dependency of Υ_S and a_S on them. We can express $(\partial Y/\partial s_i)$ and $\partial(\partial Y/\partial s_i)/\partial s_i$ (i = a, b) from Eq. (A1). For example, the first derivates are

$$\begin{aligned}\frac{\partial Y}{h_i\partial \xi_i} &= \frac{\partial Y}{\partial s_i}\\ &= \frac{1}{2}\zeta\left[Y_0'(\zeta) + (\lambda_S\Upsilon_S)Y_\Upsilon'(\zeta) + \left(\lambda_S\left(\frac{a_S'}{a_S}\right)\right)Y_a'(\zeta)\right]\\ &\quad\times\left(\frac{\partial a_S}{a_S\partial s_i}\right) + \lambda_S Y_\Upsilon(\zeta)\left(\frac{\partial \Upsilon_S}{\partial s_i}\right) + \lambda_S Y_a(\zeta)\\ &\quad\times\left(\frac{\partial a_S'}{a_S\partial s_i} - \left(\frac{a_S'}{a_S}\right)\frac{\partial a_S}{a_S\partial s_i}\right), \quad i = \text{a, b}\end{aligned}$$

These expressions and those for $\partial(\partial Y/\partial s_i)/\partial s_i$ (i = a, b) are replaced in the definition of $L_{SF}(Y)$ (i.e., in Eq. (7b)) to estimate the magnitude of $\lambda_S^2 L_{SF}(Y)$. The resulting expression is too long; therefore, we only highlight its essential features for our purpose: in addition to the terms already acknowledged as being $\sim$1, there appear $\kappa_{g,i}$ (i = a, b), Υ_S, $a_S/|a_S'|$ and the (first and second) physical derivatives of a_S', a_S and R_i (i = a, b). All these quantities appear along with factors λ_S^2 and λ_S^3 in dimensionless terms. The terms in λ_S^2 arise from $Y_0(\zeta)$ in Eq. (A1), while those in λ_S^3 arise from the remaining part of Eq. (A1).

The activity a will usually not vary too much over S_p; hence, we conservatively can assume that the scales of variation of a_S, a_S', $\partial a_S/\partial s_i$, $\partial a_S'/\partial s_i$ (i = a, b) can be at most of the same order of magnitude as the scale in the normal direction, $\Delta_a = a_S/|a_S'|$.

We have assumed before that the scale of variation of R_i in the directions ξ_a and ξ_b is $O(R_m)$. This estimate can be extended to the scale of variations of the derivatives $\partial R_i/\partial s_j$ (i = a, b; j = a, b).

We finally recall that $|\kappa_{g,i}| = O(1/R_m)$ has been previously assumed.

All these considerations along with $\lambda_S \ll R_m$ and $\lambda_S \ll a_S/|a'_S|$ (Eqs. (14d) and (15b) in the main text) allow neglecting the terms in λ_S^3 and write

$$\lambda_S^2 L_{SF}(Y) = O\left(\max\left\{\frac{\lambda_S^2}{(a_S/a'_S)^2}, \frac{\lambda_S^2}{R_m|a_S/a'_S|}\right\}\right) \tag{A2}$$

Appendix B

B.1. Evaluation of $(dY/d\zeta)_{\zeta=0}$ from Eqs. (17a)–(17c) of the main text

Considering small values of λ_S, the solution of Eqs. (17) can be expressed by a perturbation series of the form

$$Y = Y_0(\zeta) + \lambda_S Y_1(\zeta) + o(\lambda_S) \tag{B1}$$

where neither Y_0 nor Y_1 depends on λ_S. Accordingly, $r(Y)$ is expanded as

$$\begin{aligned} r(Y) &= r(Y_0) + r'(Y_0)(Y - Y_0) + \cdots \\ &= r(Y_0) + \lambda_S r'(Y_0)Y_1 + \cdots \end{aligned} \tag{B2}$$

where $r' = dr/dY$. Replacing Eqs. (B1) and (B2) into Eqs. (17) and collecting terms of zero and first order in λ_S:

$$\text{Zero order}: \quad \frac{d^2Y_0}{d\zeta^2} = r(Y_0) \tag{B3a}$$

$$\zeta = 0: \quad Y_0 = 1; \qquad \zeta \to \infty: \quad Y_0 \to 0, \quad \left(\frac{dY_0}{d\zeta}\right) \to 0 \tag{B3b}$$

$$\text{First order}: \quad \frac{d^2Y_1}{d\zeta^2} - r'(Y_0)Y_1 = \Upsilon_S \frac{dY_0}{d\zeta} + \frac{a'_S}{a_S}\zeta r(Y_0) \tag{B4a}$$

$$\zeta = 0: \quad Y_1 = 0; \qquad \zeta \to \infty: \quad Y_1 \to 0, \quad \left(\frac{dY_1}{d\zeta}\right) \to 0 \tag{B4b}$$

Terms in $(\lambda_S a'_S/a_S)^2$, $(\lambda_S \Upsilon_S)^2$, $(\lambda_S a'_S/a_S)(\lambda_S \Upsilon_S)$ and higher dimensionless terms are not being considered, so in practice the truncated solution $Y = Y_0 + \lambda_S Y_1$ will be valid for small values of $(\lambda_S a'_S/a_S)$ and $(\lambda_S \Upsilon_S)$.

The evaluation of $(dY_0/d\zeta)_{\zeta=0}$ from Eq. (B3) is well known. In what follows, it is convenient to keep in mind that Y_0 varies monotonically with ζ and therefore both, Y_0 and ζ, can be alternatively taken as the independent variable. By defining $p = dY_0/d\zeta$, Eq. (B3a) is re-written as:

$$p\left(\frac{dp}{dY_0}\right) = r(Y_0) \tag{B5}$$

By separation of variables and considering Eq. (B3b), we obtain the solution

$$p = -I(Y_0)^{1/2} \tag{B6a}$$

$$I(Y_0) = 2\int_0^{Y_0} r(Y)\,dY \tag{B6b}$$

Then

$$p(0) = \left(\frac{dY_0}{d\zeta}\right)_{\zeta=0} = -I_1 \tag{B7a}$$

$$I_1 = [I(1)]^{1/2} \tag{B7b}$$

To evaluate $(dY_1/d\zeta)_{\zeta=0}$, the left-hand side of Eq. (B4a) is expressed by:

$$\frac{d^2Y_1}{d\zeta^2} - r'(Y_0)Y_1 = \frac{d}{dY_0}\left[p\left(\frac{dY_1}{d\zeta} - \frac{dp}{dY_0}Y_1\right)\right] \tag{B8}$$

Taking into account the definition $p = dY_0/d\zeta$ and Eq. (B5), the identity (B8) can be checked by carrying out the differentiation of the square brackets.

Replacing Eq. (B8) in (B4a) and using $p = dY_0/d\zeta$ and Eq. (B5) in the right-hand side of it,

$$\frac{d}{dY_0}\left[p\left(\frac{dY_1}{d\zeta} - \frac{dp}{dY_0}Y_1\right)\right] = \Upsilon_S p + \left(\frac{a'_S}{a_S}\right)\zeta p\frac{dp}{dY_0}$$

Integrating both sides from $Y_0 = 0$ ($\zeta \to \infty$) to $Y_0 = 1$ ($\zeta = 0$) and using the boundary conditions (B4b):

$$p(0)\left(\frac{dY_1}{d\zeta}\right)_{\zeta=0} = \Upsilon_S \int_0^1 p\,dY_0 + \left(\frac{a'_S}{a_S}\right)\int_0^{p(0)} \zeta p\,dp \tag{B9}$$

Using integration by parts for the last integral:

$$\int_0^{p(0)} \zeta p\,dp = \frac{1}{2}\zeta p^2\Big|_{\zeta\to\infty}^{\zeta=0} - \frac{1}{2}\int_{\zeta\to\infty}^{\zeta=0} p^2\,d\zeta \tag{B10}$$

Since $Y_0 \to 0$ as $\zeta \to \infty$ (Eq. (B3b)), its derivative p should tend to zero faster than ζ^{-1} as $\zeta \to \infty$. Hence, we can conclude that the first term in the right-hand side of Eq. (B10) is zero. In turn, the second term can be written as:

$$-\frac{1}{2}\int_{\zeta\to\infty}^{\zeta=0} p^2\,d\zeta = -\frac{1}{2}\int_0^1 p\,dY_0$$

By substituting these results in Eq. (B9) and using Eqs. (B6a) and (B7a) for p, y, $p(0)$, we finally obtain:

$$\left(\frac{\partial Y_1}{\partial \zeta}\right)_{\zeta=0} = \left[\Upsilon_S - \frac{1}{2}\left(\frac{a'_S}{a_S}\right)\right]\frac{\int_0^1 [I(Y)]^{1/2}\,dY}{I_1} \tag{B11}$$

Taking into account Eqs. (B7a) and (B11),

$$\left(\frac{\partial Y}{\partial \zeta}\right)_{\zeta=0} \approx \left(\frac{\partial Y_0}{\partial \zeta}\right)_{\zeta=0} + \lambda_S \left(\frac{\partial Y_1}{\partial \zeta}\right)_{\zeta=0}$$
$$= -I_1 + I_2 \lambda_S \left[\Upsilon_S - \frac{1}{2}\left(\frac{a'_S}{a_S}\right)\right] \quad \text{(B12)}$$

where

$$I_2 = \frac{1}{I_1}\int_0^1 [I(Y)]^{1/2}\,\mathrm{d}Y$$

We note that in order to evaluate $(\mathrm{d}Y_1/\mathrm{d}\zeta)_{\zeta=0}$, Eq. (B11), there was no need to find out an expression for the actual profile $Y_1(\zeta)$. As regards the analysis carried out in Appendix A, it is however important quoting that Y_1 can be formally expressed as $Y_1 = \Upsilon_S Y_\Upsilon(\zeta) + (a'_S/a_S)Y_A(\zeta)$. This arises by considering that $Y_0(\zeta)$ is a function of ζ independently determined and hence, Eqs. (B4a) and (B4b) constitute a linear system for Y_1 with source terms proportional to Υ_S and (a'_S/a_S). Then, Eq. (B1) can be written as:

$$Y = Y_0(\zeta) + (\lambda_S \Upsilon_S) Y_\Upsilon(\zeta) + \left(\frac{\lambda_S a'_S}{a_S}\right) Y_a(\zeta) + o(\lambda_S) \quad \text{(B13)}$$

Besides, from Eq. (B4) it is possible to conclude that the functions $Y_\Upsilon(\zeta)$ and $Y_a(\zeta)$ will have the unity as order of magnitude.

Appendix C

C.1. Analysis of the asymptotic behaviour for multiple reactions

Conservation balances can be written at steady state for each of J reacting species $-\nabla\cdot\mathbf{N}_j = a\pi_j$ ($j = 1, \ldots, J$), where $\mathbf{N}_j$ and π_j are the flux and net consumption rate of species j, respectively. Eventually, one of these suffices can represent the heat flux and the net rate of heat consumption by the chemical reactions.

We will assume that all the species enter the catalyst from the same surface S_p, the fluxes $\mathbf{N}_j$ are related (through constitutive equations) to the physical derivatives of the concentrations C_k ($k = 1, \ldots, J$) and the rates π_j depend on C_k ($k = 1, \ldots, J$). Eventually, one of the C_j may correspond to temperature.

Assumptions (a) and (b) stated at the beginning of Section 2 in the main text are not imposed yet. In particular, this means that the concentration field may not be uniform on S_p. Also, no stoichiometric condition is imposed on the rates π_j. They can be related through a single reaction or multiple reactions.

Let us introduce dimensionless variables $c_j = C_j/C_{j,\mathrm{ref}}$, $r_j = \pi_j/\pi_{j,\mathrm{ref}}$, where the reference values $C_{j,\mathrm{ref}}$, $\pi_{j,\mathrm{ref}}$ are such that c_j and r_j will reach, and not largely exceed, values around the unity within the pellet. Proper reference values may not be those making $c_j = 1$ and $r_j = 1$ at S_p. For example, for a series reaction scheme A → B → C, both the molar concentration of B and the rate of the second reaction may be nil at the surface; therefore they are not suitable as reference values. Also, we define $\boldsymbol{F}j = \mathbf{N}_j/(D_{j,\mathrm{ref}}C_{j,\mathrm{ref}})$; where $D_{j,\mathrm{ref}}$ are reference values that represent effective diffusivities. Conservation equations become

$$-\nabla\cdot\boldsymbol{F}j = \frac{a}{\lambda_j^2} r_j, \quad j = 1, \ldots, J \quad \text{(C1)}$$

where $\lambda_j^2 = [D_j C_j/\pi_j]_{\mathrm{ref}}$. Employing the same coordinate system (ξ_a, ξ_b, ξ_n) as in the main text, the divergence in Eq. (C1) takes the form:

$$\nabla\cdot\boldsymbol{F}j = \sum_k \frac{1}{H}\frac{\partial}{\partial \xi_k}\left(\frac{H}{h_k}\boldsymbol{F}j, k\right);$$
$$H = h_a h_b h_n; \quad k = a, b, n; \quad j = 1, \ldots, J \quad \text{(C2)}$$

and $\boldsymbol{F}j, k$ is the physical component of $\boldsymbol{F}j$ in the direction ξ_k.

Assume now that chemical equilibrium is reached at a given distance (penetration depth) from the external surface, short enough to consider the pellet as a semi-infinite medium and to ignore the divergence over the surfaces parallel to S_p (i.e., the surfaces defined by ξ_n = const.). The latter assumption implies that the physical derivatives of concentrations in the directions ξ_a and ξ_b are negligible. The only significant component of the flux will be $\boldsymbol{F}_{j,n}$ (in the direction ξ_n). For general anisotropic media $\boldsymbol{F}_{j,n}$ will depend on the physical derivatives of concentrations in the three spatial directions, but as those in the directions ξ_a and ξ_b are negligible, the constitutive expression for $\boldsymbol{F}_{j,n}$ can be in practice reduced to

$$Fj, n = -\sum_{i=1}^{J} \vartheta_{ji}\left(\frac{\mathrm{d}c_i}{\mathrm{d}\xi_n}\right) = -\boldsymbol{\vartheta}_j\cdot\frac{\mathrm{d}\boldsymbol{c}}{\mathrm{d}\xi_n} \quad \text{(C3)}$$

where $\boldsymbol{c} = (c_1, \ldots, c_J)^{\mathrm{T}}$ and $\boldsymbol{\vartheta}_j = (\boldsymbol{\vartheta}_{j1}, \ldots, \boldsymbol{\vartheta}_{jJ})^{\mathrm{T}}$ is a vector of dimensionless transport coefficients (generically dependent on $\boldsymbol{c}$ and position).

It is assumed that values $D_{j,\mathrm{ref}}$ have been defined in such a way that the order of magnitude of the largest coefficient ϑ_{ji} for each j is the unity. Defining $\lambda = \max\{\lambda_j\}$ and, for a local value of a_S, $\lambda_S = \lambda/a_S^{1/2}$, the penetration depth and λ_S will be of the same order of magnitude, if the reference values $C_{j,\mathrm{ref}}$, $\pi_{j,\mathrm{ref}}$, $D_{j,\mathrm{ref}}$ have been properly chosen. For the conditions stated above, Eq. (C2) is reduced to the following 1D problem locally defined:

$$\frac{1}{(1-\zeta\lambda_S\kappa_a)(1-\zeta\lambda_S\kappa_b)} \times \frac{\mathrm{d}}{\mathrm{d}\zeta}\left((1-\zeta\lambda_S\kappa_a)(1-\zeta\lambda_S\kappa_b)\boldsymbol{\vartheta}_j\cdot\frac{\mathrm{d}\boldsymbol{c}}{\mathrm{d}\zeta}\right) = a^* \upsilon_j r_j \quad \text{(C4)}$$

where (stretched variable) $\zeta = \xi_n/\lambda_S$, $\upsilon_j = (\lambda/\lambda_j)^2$ and with the boundary conditions:

$$\zeta = 0: \quad \boldsymbol{c} = \boldsymbol{c}_S \quad \text{(C5a)}$$

$$\zeta \to \infty : \quad \frac{\mathrm{d}\boldsymbol{c}}{\mathrm{d}\zeta} = 0 \tag{C5b}$$

The dimensionless activity a^* is defined in the same way as in the main text and expressed according to expression (15a),

$$a^* = 1 + \left(\frac{a'_\mathrm{S}}{a_\mathrm{S}}\right)\zeta\lambda_\mathrm{S} + \frac{1}{2}\left(\frac{a''_\mathrm{S}}{a_\mathrm{S}}\right)(\zeta\lambda_\mathrm{S})^2 + \cdots \tag{C6}$$

Consider for λ_S restrictions similar to those introduced in the main text (Eqs. (14d) and (15b)),

$$\lambda_\mathrm{S} \ll R_\mathrm{m}, \qquad \lambda_\mathrm{S} \ll \left|\frac{a_\mathrm{S}}{a'_\mathrm{S}}\right| \tag{C7}$$

As in the case of a single reaction, the condition $\mathrm{d}\boldsymbol{c}/\mathrm{d}\zeta = 0$ in Eq. (C5b) will be already reached for practical purposes when ζ reaches a few units, provided that Eq. (C7) are satisfied. In addition, we can neglect the terms in $(\zeta\lambda_\mathrm{S})^2$ in Eqs. (C4) and (C6). Then, Eq. (C4) becomes after rearranging

$$\frac{\mathrm{d}}{\mathrm{d}\zeta}\left(\boldsymbol{\vartheta}_j \cdot \frac{\mathrm{d}\boldsymbol{c}}{\mathrm{d}\zeta}\right) - \frac{\lambda_\mathrm{S}\Upsilon_\mathrm{S}}{1-\zeta\lambda_\mathrm{S}\Upsilon_\mathrm{S}}\boldsymbol{\vartheta}_j \cdot \frac{\mathrm{d}\boldsymbol{c}}{\mathrm{d}\zeta} \approx [1 - 2\lambda_\mathrm{S}A_\mathrm{S}\zeta]\upsilon_j r_j \tag{C8}$$

where $\Upsilon_\mathrm{S} = \kappa_\mathrm{a} + \kappa_\mathrm{b}$ and $A_\mathrm{S} = -(1/2)a'_\mathrm{S}/a_\mathrm{S}$. We should keep in mind that in Eq. (C8) and in the rest of equations in this appendix the sign "≈" means that terms of lower order of magnitude have been neglected.

Considering that the second term of the left-hand side in Eq. (C8) is already of an order of magnitude less than the first term, we can approximate $(1 - \zeta\lambda_\mathrm{S}\Upsilon_\mathrm{S}) \cong 1$. Then,

$$\frac{\mathrm{d}}{\mathrm{d}\zeta}\left(\boldsymbol{\vartheta}_j \cdot \frac{\mathrm{d}\boldsymbol{c}}{\mathrm{d}\zeta}\right) - \lambda_\mathrm{S}\Upsilon_\mathrm{S}\boldsymbol{\vartheta}_j \cdot \frac{\mathrm{d}\boldsymbol{c}}{\mathrm{d}\zeta} \approx [1 - 2\lambda_\mathrm{S}A_\mathrm{S}\zeta]\upsilon_j r_j \tag{C9}$$

It is interesting to mention that for Eq. (C9) (or (C4)) the fluxes $N_{j,n} = F_{j,n}(D_{j,\mathrm{ref}}C_{j,\mathrm{ref}})$ keep the same stoichiometric relationships as the rates π_j do, a condition that holds from the unidirectional nature of the problem, along with conditions (C5). By considering the stoichiometric relationships for a single reaction and the fluxes defined as in Eq. (C3), the procedure outlined in Section 2 of the main text can be carried out to obtain, at the end, the parameter J_A (Eq. (1d)) and the relationships between the concentration of the different species and variable Y. Then, it will be possible to recognize that Eq. (17a) is a special case of Eq. (C9).

It is obvious that in Eq. (C9) the quantities Υ_S and A_S do not occur in an additive way. The same happened with the equivalent equation (17a) in the main text. However, the procedure followed in Appendix B to obtain the flux at S_p from Eq. (17a) led to conclude that the main effects of both parameters take place additively, i.e., $N_{AS,\mathrm{high}}$ depends on $(\Upsilon_\mathrm{S} + A_\mathrm{S})$, Eq. (18) in the main text. Unfortunately, the whole procedure in Appendix B cannot be followed one-to-one for multiple reactions (because there is more than one independent state variable). Nonetheless, it is still possible to transform Eq. (C9) and confirm that for multiple reactions both parameters also exert their main effects additively.

To this end, note that on account of the small values assumed for $\lambda_\mathrm{S}A_\mathrm{S}$ the approximation $\exp(-2\zeta A_\mathrm{S}\lambda_\mathrm{S})$ is as precise as $[1 - 2A_\mathrm{S}\lambda_\mathrm{S}\zeta]$ for the activity term. Hence, we can write alternatively from Eq. (C9)

$$\frac{\mathrm{d}}{\mathrm{d}\zeta}\left(\boldsymbol{\vartheta}_j \cdot \frac{\mathrm{d}\boldsymbol{c}}{\mathrm{d}\zeta}\right) - \lambda_\mathrm{S}\Upsilon_\mathrm{S}\boldsymbol{\vartheta}_j \cdot \frac{\mathrm{d}\boldsymbol{c}}{\mathrm{d}\zeta} \approx \exp(-2\zeta\lambda_\mathrm{S}A_\mathrm{S})\upsilon_j r_j \tag{C10}$$

The following change of variables is now employed:

$$\tilde{\zeta} = \frac{1 - \exp(-\zeta\lambda_\mathrm{S}A_\mathrm{S})}{\lambda_\mathrm{S}A_\mathrm{S}} \tag{C11}$$

Hence, Eq. (C10) turns into

$$\frac{\mathrm{d}(\boldsymbol{\vartheta}_j \cdot (\mathrm{d}\boldsymbol{c}/\mathrm{d}\tilde{\zeta}))}{\mathrm{d}\tilde{\zeta}} - \frac{\lambda_\mathrm{S}(\Upsilon_\mathrm{S} + A_\mathrm{S})}{1 - \tilde{\zeta}\lambda_\mathrm{S}A_\mathrm{S}}\boldsymbol{\vartheta}_j \cdot \frac{\mathrm{d}\boldsymbol{c}}{\mathrm{d}\tilde{\zeta}} \approx \upsilon_j r_j \tag{C12}$$

Considering restrictions (C7) and the transformation (C11), variables $\tilde{\zeta}$ and ζ will be very similar to each other up to values of around unity. Then, taking $(1 - \tilde{\zeta}\lambda_\mathrm{S}A_\mathrm{S}) \approx 1$ in Eq. (C12) will not change the precision of the results and we finally obtain:

$$\frac{\mathrm{d}(\boldsymbol{\vartheta}_j \cdot \mathrm{d}\boldsymbol{c}/\mathrm{d}\tilde{\zeta})}{\mathrm{d}\tilde{\zeta}} - \lambda_\mathrm{S}(\Upsilon_\mathrm{S} + A_\mathrm{S})\boldsymbol{\vartheta}_j \cdot \frac{\mathrm{d}\boldsymbol{c}}{\mathrm{d}\tilde{\zeta}} \approx \upsilon_j r_j \tag{C13}$$

From Eq. (C11), when $\zeta = 0$: $\tilde{\zeta} = 0$. When $\zeta \to \infty$: $\tilde{\zeta} \to$ "a large value" [∞ if $A_\mathrm{S} < 0$, $(\lambda_\mathrm{S}A_\mathrm{S})^{-1}$ if $A_\mathrm{S} > 0$]. Therefore, accounting for Eqs. (C5), we can take in practice the following boundary conditions for Eq. (C13)

$$\tilde{\zeta} = 0 : \quad \boldsymbol{c} = \boldsymbol{c}_\mathrm{S} \tag{C14a}$$

$$\tilde{\zeta} \to \infty : \quad \frac{\mathrm{d}\boldsymbol{c}}{\mathrm{d}\tilde{\zeta}} = 0 \tag{C14b}$$

We can also conclude from Eq. (C11) that $(\boldsymbol{\vartheta}_j \cdot \mathrm{d}\boldsymbol{c}/\mathrm{d}\zeta)_{\zeta=0} = (\boldsymbol{\vartheta}_j \cdot \mathrm{d}\boldsymbol{c}/\mathrm{d}\tilde{\zeta})_{\tilde{\zeta}=0}$. Therefore, the solution of Eqs. (C13) and (C14) will directly allow the evaluation of the fluxes at S_p. Eq. (C13) is the desired result concerning the sum $(A_\mathrm{S} + \Upsilon_\mathrm{S})$.

A perturbation analysis, similar to that employed in Appendix B for a single reaction, can be formally set out for Eq. (C13), by taking $[\lambda_\mathrm{S}(A_\mathrm{S} + \Upsilon_\mathrm{S})]$ as the perturbation parameter. The solution will show the form:

$$\boldsymbol{c} = \boldsymbol{c}_0(\tilde{\zeta}) + \boldsymbol{c}_1(\tilde{\zeta})\lambda_\mathrm{S}(A_\mathrm{S} + \Upsilon_\mathrm{S}) + \cdots \tag{C15}$$

where $\boldsymbol{c}_0$, $\boldsymbol{c}_1$ will also depend on kinetic and transport parameters and on $\boldsymbol{c}_\mathrm{S}$. The value $(\boldsymbol{\vartheta}_j \cdot \mathrm{d}\boldsymbol{c}/\mathrm{d}\tilde{\zeta})_{\tilde{\zeta}=0}$ follows from Eq. (C15), and $N_{j\mathrm{S},\mathrm{high}} = D_{j,\mathrm{ref}}C_{j,\mathrm{ref}}(1/\lambda_\mathrm{S})(\boldsymbol{\vartheta}_j \cdot \mathrm{d}\boldsymbol{c}/\mathrm{d}\tilde{\zeta})_{\tilde{\zeta}=0}$ can be evaluated and expressed as:

$$N_{j\mathrm{S},\mathrm{high}} = D_{j,\mathrm{ref}}C_{j,\mathrm{ref}}\left[\frac{1}{\lambda}I_{1,j}a_\mathrm{S}^{1/2} - I_{2,j}(\Upsilon_\mathrm{S} + A_\mathrm{S})\right] \tag{C16}$$

where the coefficients $I_{1,j}$ and $I_{2,j}$ depend on kinetic and transport properties and on $\boldsymbol{c}_\mathrm{S}$.

We recall at this point that assumptions (a) and (b) stated in Section 2 of the main text are not required for Eqs. (C13)–(C16) to hold. Eqs. (C13) and (C14) can be solved

on a local basis over S_p to obtain $N_{jS,\text{high}}$, which can be integrated afterwards.

Instead, to obtain expressions like Eq. (22) in the main text for $R_{j,\text{high}}$, we should impose assumptions (a) and (b) that allow $I_{1,j}$ and $I_{2,j}$ (Eq. (C16)) to be uniform on S_p. Then, by integrating $N_{jS,\text{high}}$ over S_p and using definitions (20) and (21) in the main text

$$R_{j,\text{high}} = \frac{D_{j,\text{ref}} C_{j,\text{ref}} S_p (a_S^{1/2})_{\text{av}} I_{1,j}}{\lambda} \left[1 - \frac{I_{2,j}}{I_{1,j}} \frac{\lambda}{\ell} \Gamma \right], \quad j = 1, \ldots, J \tag{C17}$$

Thus, Eq. (C17) clearly shows that the second order correction in $R_{j,\text{high}}$ depends, as regards activity profiles and geometry, on the same parameter Γ as for the case of a single reaction (cf. Eq. (22) in the main text).

The coefficients $I_{1,j}$ and $I_{2,j}$ will no longer available in a close way and should be evaluated numerically. However, the following way is better for actual computations of $R_{j,\text{high}}$. Dividing Eq. (C17) by S_p and rearranging

$$\frac{R_{j,\text{high}}}{S_p} = (N_{jS,\text{high}})_{\text{av}} = D_{j,\text{ref}} C_{j,\text{ref}} \left[\frac{1}{\lambda} I_{1,j} (a_S^{1/2})_{\text{av}} - I_{2,j} (\Upsilon_S + A_S)_{\text{av}} \right] \tag{C18}$$

Recalling the relation between Eqs. (C13) and (C16), we can appreciate from Eq. (C18) that $(N_{jS,\text{high}})_{\text{av}}$ (and hence $R_{j,\text{high}}$) can be computed from the numerical solution of Eq. (C13) with $\lambda_S \equiv \lambda/(a_S^{1/2})_{\text{av}}$ and $(\Upsilon_S + A_S) \equiv (\Upsilon_S + A_S)_{\text{av}}$.

We finally mention that an alternative way to express Eq. (C13) is by collecting the terms in the left-hand side:

$$\frac{\mathrm{d}[S(\tilde{\zeta})(\boldsymbol{\vartheta}_j \cdot \mathrm{d}\boldsymbol{c}/\mathrm{d}\tilde{\zeta})]}{S(\tilde{\zeta})\,\mathrm{d}\tilde{\zeta}} \approx \upsilon_j r_j, \quad S(\tilde{\zeta}) = \mathrm{e}^{-\lambda_S(\Upsilon_S + A_S)\tilde{\zeta}} \tag{C19}$$

Eq. (C19) clearly describes 1D diffusion and reaction in a (hypothetical) catalytic body with cross-section area varying according to $S(\tilde{\zeta})$.

References

[1] R. Aris, The Mathematical Theory of Diffusion and Reaction in Permeable Catalysts, Oxford University Press, London, 1975.

[2] D. Papadias, L. Edsberg, P. Björnbom, Simplified method for effectiveness factor calculations in irregular geometries of washcoats, Chem. Eng. Sci. 8 (55) (2000) 1447–1459.

[3] S. Wedel, D. Luss, A rational approximation of the effectiveness factor, Chem. Eng. Commun. 11 (1980) 245–259.

[4] E.E. Gonzo, J.C. Gottifredi, Rational approximation of effectiveness factor and general diagnostic criteria for heat and mass transport limitations, Catal. Rev. Sci. Eng. 25 (1) (1983) 119–140.

[5] N.J. Mariani, S.D. Keegan, O.M. Martínez, G.F. Barreto, A one-dimensional equivalent model to evaluate overall reaction rates in catalytic pellets, Chem. Eng. Res. Des. 81 (Part A) (2003) 1033–1042.

[6] A. Cybulski, J.A. Moulijn, Structured Catalysts and Reactors, Marcel Dekker, New York, 1998.

[7] W.E. Stewart, Invariant solutions for steady diffusion and reaction in permeable catalysts, Chem. Eng. Sci. 33 (1978) 547–553.

[8] A. Burghardt, Transport phenomena and chemical reactions in porous catalysts for multicomponent and multireaction systems, Chem. Eng. Process 21 (1986) 229–244.

[9] E. Kreyszig, Differential Geometry, University of Toronto Press, Toronto, 1959.

[10] B.A. Buffham, The size and compactness of particles of arbitrary shape: application to catalyst effectiveness factors, Chem. Eng. Sci. 55 (2000) 5803–5811.

[11] R.E. Hayes, B. Liu, R. Moxom, M. Votsmeier, The effect of washcoat geometry on mass transfer in monolith reactors, Chem. Eng. Sci. 59 (2004) 3169–3181.

[12] B.M. Gillespie, E.D. Crandall, J.J. Carberry, Local and average interphase heat transfer coefficients in a randomly packed bed of spheres, AIChE J. 14 (3) (1968) 483–490.